



CHAPTER III

CHARACTERISATION OF PHOSPHORS

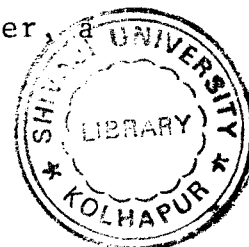


3.1 Introduction :

This chapter gives detailed information regarding the structural, electrical, magnetic and optical characterisation of SrSO_4 phosphors, prepared in the present study. The characterisation of phosphor before undertaking any luminescence studies is indispensable. Such studies help to understand the mechanism of emission of light in the phosphor system under investigation. The luminescence properties mainly depend on the crystal structure, the type of impurity doped and the amount of impurity actually gone in the lattice during preparation of the phosphors. In the present investigation an attempt has been made to characterise the phosphors on the basis of structural, electrical, magnetic and optical properties.

3.2 Structural Characterisation :

X-ray diffraction studies are used for identification of Solid Crystalline Substances. The basis of the studies is that each substance gives a characteristic X-ray pattern and no two chemically distinct substances give identical patterns. The positions of lines and their relative intensities do not vary appreciable under given experimental conditions. If the structure of material is known its diffraction pattern can be evaluated in a very straight forward manner. However,



direct calculation of structure of substance from the observed pattern can never be evaluated, if the structure of starting material is not known.

In the present investigation the XRD study was carried out on philips PW-1051 X-ray diffractometer. The X-ray machine was operated on 35 KV, 40 mA, using $\text{CuK}\alpha$ radiations with wavelength $\lambda = 1.54178 \text{ \AA}$. Scanning rate was 5 mm/ Degree. The XRD patterns for the phosphors were recorded within the span of angles between 10° to 90° . The rate of meter and chart speed were kept constant for all the runs.

The X-ray diffraction patterns for typical phosphors SC_{00} , SC_{01} , SC_{03} , SC_{11} and SC_{38}^* were obtained and are depicted in fig. 3.1 and 3.2. Before obtaining XRD patterns, these phosphors were ground in an agate mortar and sieved through a 325 mesh screen to get, the particles of uniform size.

The fig. 3.1 and 3.2 were used to calculate the values of 2θ (degree) and the corresponding relative intensity 'I' (Arb. Units) for the respective phosphors; and the values so obtained are presented in Table No. 3.1 to 3.5. The interplaner distances 'd' have been calculated by using well known Bragg's relation and these values were compared with standard values of 'd' from ASTM card No. 5-0593 (Page - 821). The comparision makes

it possible to obtain 'h', 'k' and 'l' values for the planes in the crystal under study. The calculated 'd', observed 'd' (from ASTM Card) and (h, k, l) values for five different phosphors are presented in Table No. 3.1 to 3.5. From tables it can be noted that the values of calculated 'd' and observed 'd' are in agreement with each other.

It is well known that the structure of the starting material (SrSO_4), used in the present investigation, is orthorhombic¹; with lattice parameters -

$$a_0 = 8.539 \pm 0.005 \text{ \AA}, \quad b_0 = 5.352 \pm 0.005 \text{ \AA} \text{ and}$$

$c_0 = 6.866 \pm 0.005 \text{ \AA}$. Hence in the present investigation, for calculation of lattice parameters for $\text{SrSO}_4:\text{Dy}$ and $\text{SrSO}_4:\text{Tb}$, the formula

$$\frac{1}{d^2} = \frac{h^2}{a_0^2} + \frac{k^2}{b_0^2} + \frac{l^2}{c_0^2}$$

is used. The suitable planes were choosed by trial & error method. The calculated values of lattice parameters for SC_{01} , SC_{03} , SC_{11} and SC_{38}^* are given in the tables - (Table 3.2 to 3.5). The comparision of the calculated values of lattice parameters with standard values renders to suggest that the structure of prepared phosphors is also orthorhombic¹ and there is no change in the structure even after doping with the activators with and without the charge compensator.

Further from Fig. 3.1 it can be noted that the peak positions of starting material (SC_{00}), heat treated $SrSO_4$ (SC_{01}) and Dy added $SrSO_4$ (SC_{03}) possesses one to one similarity. This confirms that the incorporation of activator does not bring about appreciable change in the crystal structure. This appears to suggest that a traps in the present phosphor system are due to host lattice defects, rather than activator added. Similar contention has been more clearly investigated by other workers for alkaline earth sulphate phosphors,^{2,3,4}. The comparison of relative intensities of heat treated $SrSO_4$ (SC_{01}) and Dy added $SrSO_4$ (SC_{03}) (Fig. 3.1) shows that relative intensity gets increased by the addition of activator.

Fig. 3.2 gives X-ray diffraction pattern with (SC_{38}^*) and without (SC_{11}) Na_2SO_4 added $SrSO_4:Tb$ phosphors. It can be noted from fig. 3.2, that peak positions are same, for both the phosphors similar to that obtained for $SrSO_4 : Dy$ phosphors. (Fig. 3.1). This shows that the addition of Na_2SO_4 during the preparation of phosphor can not be suspected to give rise a new compound. The comparison of relative peak intensities of $SrSO_4:Tb$ phosphors with (SC_{38}^*) and without (SC_{11}) Na_2SO_4 shows that, the peak heights of Na_2SO_4 added phosphors have been increased as per expectation. The addition of Na_2SO_4 helps only to incorporate more number of trivalent activator ions like -

9613

A

Tb^{3+} in to the host lattice for charge compensation. The increased population of Tb^{3+} or Dy^{3+} ions in Na_2SO_4 added $SrSO_4$ (SC_{38}^*) phosphor is explained at length in forth coming chapter. The comparision of peak intensity at around $2\theta = 42.2^\circ$, for with (SC_{38}^*) and without (SC_{11}) Na_2SO_4 added phosphor appears to indicate that plane corresponding to $2\theta = 44.2^\circ$ is favourable plane for incorporation of Tb^{3+} ions along with Na^+ ion in the host lattice. In addition to the prominent peaks, the spikes with low intensity can be seen to be present in the X-ray diffraction pattern (Fig. 3.1 and 3.2). This might be due to the noise in the detection system of X-ray diffractometer or due to the traces of impurities present in the starting material. Similar results were reported by Rao⁵ for alkaline earth sulfide phosphors.

Thus the principle findings of structural characterisation may be summarised as follows.

1. The structure of $SrSO_4:Dy$ and $SrSO_4:Tb$ phosphors with and without Na_2SO_4 is orthorhombic.
2. The addition of activator ion (Dy^{3+} or Tb^{3+}) along with Na^+ ion appears to increase the population of activator ion in $SrSO_4$ phosphors.

3.3 Electrical Characterisation :

3.3.1 A.C. Conductivity

In order to obtain the information regarding the conductivity of prepared phosphors, the variation of

current (I) through electroluminescent cell with the applied voltage, has been measured for various phosphors. The nature of I-V curves for almost all the phosphors is similar. In order to avoid repeatation, typical I-V plots are shown in fig. 3.3 & 3.4. From the graph it can be seen that I versus V plots are not exactly linear. To understand nature of I-V curves, the graph of log I is plotted against logV and they are as shown in fig. 3.5. It can be seen that the plots are linear with slope nearly equal to 2 and hence I-V curves can be fitted in the relation⁶.

$$I = (9 \mu V^2) / (32 \pi L^3)$$

Where, V = Voltage drop across the phosphor system.
 μ = Mobility of the charge carrier
 I = Current flowing through the E.L. cell.
 L = Thickness of thin uniform layer of micro crystalline powder (thickness 0.02 cm) in electroluminescent cell.

The I-V characteristics are observed to be non-linear for low and high voltages (Fig. 3.3 and 3.4). However in the voltage range 400 to 1000 volts they are found to be linear. The slopes of linear portion of I-V characteristics gives electrical conductance of phosphors.

In the present investigation the electrical conductance of SrSO_4 phosphors with diverse concentration of Dy or Tb at room temperature are measured and they are listed in table no. 3.6. From table no. 3.6 and from fig. 3.3 and 3.4 following points are worth noting.

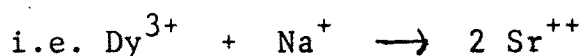
1. The electrical conductance of SrSO_4 : Tb phosphors without Na_2SO_4 decreases with the increase of concentration of Tb similar result is obtained for SrSO_4 : Dy phosphors.
2. The electrical conductance of SrSO_4 : Dy phosphors without Na_2SO_4 gives more electrical conductance than with Na_2SO_4 phosphors. Similar results are obtained for SrSO_4 :Tb phosphors.

The decrease in the electrical conductivity of SrSO_4 phosphors with addition of Dy^{3+} or Tb^{3+} ions may be attributed to the scattering of charge carriers due to the Dy or Tb impurities. Such a decrease in conductivity has been observed in silver halides with Cd^{7+} and in sodium nitrate doped with barium⁸.

The decrease of electrical conductance of Na_2SO_4 added SrSO_4 phosphors may be understood as follows : The addition of 2Dy^{3+} ions in the matrix of SrSO_4 can replace 3Sr^{++} ions creating one cation vacancy to preserve the charge Neutrality in without Na_2SO_4 added phosphors.



However when a trivalent impurity ion Dy^{3+} is doped along with a monovalent impurity ion Na^+ , they do not create any vacancy.



This suggest that incorporation of Dy^{3+} along with Na^+ in SrSO_4 matrix decreases the no. of cation vacancy, which results in decreasing the conductivity.

3.3.2 D.C. Resistivity

Attempt was made to determine the d.c. resistivity of some typical phosphors whose pellets were prepared, by compacting the polycrystalline powder. Initially acetone was mixed in the powder phosphor and Polyvelene acetate was used as a binder. The mixture was, dried and crushed with agate mortar. The mixture was then put into a dia of 1cm. diameter under constant pressure of 7 tones/inch² with the help of hydraulic press, for 15 minutes at room temperature. (300° K).

The apparatus for the resistivity measurement is depicted in fig. 3.6. The pellete was mounted between circular brass electrode and d.c. voltage is applied to the sample up to 350 volts. The current was measured by applying different d.c. voltages. Auto range digital multimeter meco model 6E was used to measure the current. Then, for the sample which is in the form of pellete,

resistivity is given by

$$\rho = (A/I) \cdot (V/d)$$

Where 'A' is cross sectional area of pellete, 'I' is current passing through pellete for the voltage 'V' and 'd' is thickness of pellete. The graph of current verses voltage is plotted for three typical phosphors, SC_{01} , SC_{03} and SC_{30}^* (fig. 3.7) from which d.c. resistivity was calculated .

The d.c. resistivity for heat treated $SrSO_4$ (SC_{01}) was found to be $327.28 \text{ m}\Omega$, while for $SrSO_4:0.1 \text{ Wt.}\% \text{ Dy}$ (SC_{03}) phosphor it is $20.455 \text{ m}\Omega$ & for $SrSO_4:0.1 \text{ Wt.}\% \text{ Dy}$ with Na_2SO_4 (SC_{30}^*), it is found to $163.64 \text{ m}\Omega$. These results can be explained as follows.

Heat treated $SrSO_4$ (SC_{01}) phosphor gives high resistivity. This is because in the preparation of phosphor few vacancies might have been created which are responsible for giving small conductivity i.e. high resistivity for this sample. The resistivity of SC_{03} phosphor has decreased because in the preperation of phosphor 2 Dy^{3+} ions replaces 3 Sr^{++} ions as a result there is formation of + Ve ion vacancy which acts as a charge carrier. The resistivity of SC_{30} phosphor has increased.. This is because Dy^{3+} ions along with one Na^+ ion can replaces 2 Sr^{++} ions. Hence addition of Na_2SO_4 in $SrSO_4 : Dy$ phosphor decreases the + ve ion

vacancy in the phosphor. Naturally conductivity decreases and resistivity increases as per the expectation.

3.3.3 Thermoelectric Power

Thermoelectric Power measurements enables to understand the nature of prepared phosphors, whether p - type or n - type. The thermoelectric power is the ratio of thermally generated Voltage to the temperature difference across the semi-conductor. The temperature difference across the semiconductor causes the migration of majority charge carriers. In the steady state electric field is established which gives rise to open circuit voltage called as thermoelectric Voltage, which is proportional to the temperature difference across the phosphor system. In case of Ionic Solid thermoelectric power is due to the diffusion of vacancies or Interstitials and is given by the expression⁹.

$$\alpha = -\frac{k}{q} (2\epsilon - 1) \frac{\Delta H}{kT} - \ln(\nu/\nu')^{3Z} + \ln \frac{c}{1-c} \int_0^T c_p \frac{m dT}{kT}$$

where α is thermoelectric power, ν' is the frequency of neighbouring ions on a vacancy, 'Z' is the no. of nearest neighbours, ΔH is the activation energy for Jumping process, $\epsilon \cong 1$ for vacancy diffusion and 1/2 for interstitial diffusion.

In the present investigation thermoelectric power of some typical phosphors SC_{01} , SC_{02} , SC_{03} , SC_{30}^* ,

SC_{11} and SC_{40}^* prepared in the form of pellete was measured. The formation of the pellets is described in section 3.3.2

The schematic diagram of the experimental set-up used for thermoelectric power measurement is shown in fig. 3.8. The apparatus consisted of two brass electrodes. The lower electrode was heated by passing current through the heating coil, which is wound inductively on the lower electrode and heating coil are electrically insulated from each other by placing the insulating material between them. The temperature of lower electrode can be varied by changing the current through heating coil with the help of dimmerstat. The lower electrode and heating coil are surrounded by the metal cover. The temperature of lower electrode was measured with the help of chromel - Alumel thermocouple. The temperature of upper electrode is also measured with the help of chromel - Alumel thermocouple of 26 S.W.G. The upper electrode is kept at constant temperature i.e. at room temperature.

The Phosphor which is in the form of pellete was coated with silver paint and was employed for thermoelectric power measurements. The pellete was kept between upper and lower electrode and was heated by

passing the current through heating coil on lower electrode. The thermoemf. generated between two brass electrodes is measured with the help of Aplab, microvoltmeter.

The maximum thermoelectric power for $\text{SrSO}_4:\text{Dy}$ phosphor was observed to be $3.266 \text{ mv}/^\circ\text{C}$ and it was found to vary linearly with temperature in the temperature range 30°C to 300°C . The generation of thermoelectric power may be attributed to the presence of more cation vacancies formed during the preparation of phosphor. Further in the measurement of thermoelectric power for all the pellets, it was found that the polarity developed across pellet is + Ve at the cold junction. This might be due to the presence of Sr^{++} vacancies in the present phosphor system. The observations of thermoelectric power measurements reveals that the phosphor material prepared in the present investigation is of P - type. Similar observations have been reported by Jagdale¹⁰ for CaSO_4 Phosphor.

3.4 Magnetic Characterisation :

a. Magnetic Behaviour of SrSO_4 Phosphors

It is interesting to study the magnetic properties of these phosphors, because doped atom has its shell partly filled with electron, and the electrons of the unfilled shell provide net magnetic moments and

accounts for the magnetic properties of these ions in solids. It is believed that the susceptibility change is a property of the difference in magnetic character of unexcited and trapped electrons.

In the past Jensen¹¹ has measured paramagnetic susceptibility of trapped electrons in alkali halides. Bowers and Melamed¹² have reported the temperature dependence of magnetic susceptibility of Cu- activated Zns, while Johnson and Williams^{13,14} have studied change in susceptibility of Mn activated ZnF_2 phosphors after radiating excitation. Mulla and Pawar¹⁵ have studied the magnetic behaviour of $CaSO_4$ phosphors.

In the present investigation, with the view to understand the behaviour of Dy^{3+} and Na^+ ion in $SrSO_4$ lattice, attempts have been made to measure the magnetic susceptibility of these phosphors with the special interest, to know the effects of charge compensation in these phosphors.

b. Magnetic Susceptibility Measurements

There are various methods of measuring the susceptibilities of solids and these methods can be classified as uniform field and non uniform field methods. The important aspects of these methods such as applicability, limitations etc. have been summarised by

Mulay¹⁶. In the present study Gouy method is used which falls in the category of uniform field method, developed by French physicist Gouy¹⁷. The experimental arrangement used is photographed in fig. 3.9. In this method the specimen is Gouy tube, is suspended from one arm of sensitive balance. The lower end of the specimen is placed between the poles of an electromagnet which gives well defined and extremely uniform field. When the magnet is energised, the specimen experiences a force which pulls it further in to the field if the substance is paramagnetic and pushes it out of the field, if it is diamagnetic. Initially weights are added in the pan such that deflection must be within scale. Then by changing various values of current various deflections are measured. The change in deflection gives the magnitude of force 'Fs', which acts vertically on the specimen and it can be shown that,

$$F_s = \frac{1}{2} K_s A H^2 \quad \dots\dots\dots (1)$$

Where 'A' is the cross-section of the specimen, and 'H' is the strength of the uniform field and F_s is the volume susceptibility of the specimen. If we consider the atmosphere surrounding, the Gouy tube which has a susceptibility K_o and the field at the other end $H_o = 0$, the equation (1) becomes

$$F_s = \frac{1}{2} (K_s - K_o) H^2 A \quad \dots\dots\dots (2)$$

The experimental arrangement enables to measure the force directly.

$$\text{Hence, } F_s = m_s g = \frac{1}{2} (K_s - K_o) H^2 A \quad \dots\dots(3)$$

Where, m_s is change in weight of phosphor.

Similar equation for standard reference liquid in Gouy tube can be written as -

$$F_r = m_r g = \frac{1}{2} (K_r - K_o) H^2 A \quad \dots\dots (4)$$

Where, K_r and m_r are the corresponding quantities for reference liquid. Equation (3) & (4) yeilds -

$$K_s = \frac{m_s}{m_r} (K_r - K_o) + K_o \quad \dots\dots\dots (5)$$

This is well known relation for the measurement of magnetic susceptibility of the material.

The Gouy method is perticularly suited for the measurement of diamagnetic and paramagnetic susceptibilities of samples obtained in the form of powdered solids, liquids and solutions and in all these cases Gouy's method provides a measurement of volume susceptibility. Experimental set up used for measurement of susceptibility consists a semi-micro balance capable of measuring up to 1×10^{-5} gram was used to measure the force on the phosphor contained in a thin walled pyrex tube of 5 mm diameter and 15 cm in length. Small and nearly equal

amounts of the powder was introduced in the tube and packed by pounding after each successive addition with the flat end of a ram rod, that snugly fits the tube. The experimental procedure eliminated the observed forces on the pyrex tube arising from certain paramagnetic impurities¹⁸ as well as change in bouyancy of air.

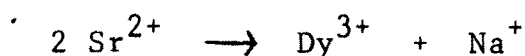
The magnetic field of the order of 7.5 koe was applied. The distance between the pole pieces was kept constant equal to 3 cm. The reference liquid used was benzene. The magnetic susceptibility K_r of which is -0.611×10^{-6} . The magnetic susceptibilities of $\text{SrSO}_4:\text{Dy}$ and $\text{SrSO}_4:\text{Tb}$ were estimated by using the relation (5).

c. Results and Discussion

The magnetic susceptibilities of $\text{SrSO}_4:\text{Dy}$ phosphors with and without the addition of Na_2SO_4 have been measured and the graph of magnetic susceptibility is plotted for diverse activator concentration of Dy for some typical phosphors and it is shown in fig. 3.10. It can be noted that the magnetic susceptibilities of these phosphors vary non linearly with the composition in contrast to the Langivans diamagnetic theory. Similar observation have been reported by Mulla and Pawar⁸ for $\text{CaSO}_4:\text{Dy}$ phosphor. From the curve (Fig. 3.10) it can be noted that there is increase in the magnetic susceptibility in the + ve direction with the increase in the activator concentration this can be understood as follows.

In the present investigation phosphors were prepared in the atmosphere of H_2SO_4 and it is most likely that there are number of Sr^{2+} vacancies or excess SO_4^{2-} radicals which acts as paramagnetic species¹⁹. Further it is well known that Dy^{3+} is paramagnetic in nature and naturally its entry in the host lattice should make the system more paramagnetic. It is evident that the concentration of paramagnetic ion in SrSO_4 lattice is increasing with the increase in concentration of Dy, therefore, this may give rise to an increase in the magnetic susceptibility, for higher concentration of Dy in the SrSO_4 phosphors. In the process of incorporating more and more Dy ions it is likely that 2 Dy^{3+} can be introduced in the host lattice by removing 3 Ca^{2+} ions under the condition of charge balancing, leaving behind SO_4^{2-} radical. The ESR study of irradiated SrSO_4 rare-earth phosphor shows the presence of SO_4^{2-} radical which are paramagnetic in nature.

From the fig. it can be noted that Na_2SO_4 added phosphors are less diamagnetic this can be explained on the basis of charge compensation theory of Kroger and Helligmann. According to Charge compensation theory of Kroger and Helligmann, Na^+ ion from Na_2SO_4 makes an easy entry of Dy^{3+} in SrSO_4 , by removing 2 Sr^{2+} ions the charge balancing occurs as follows,



Hence more number of Dy ions can be introduced in the process of charge compensation. However in without charge compensator phosphors two ions of DY^{3+} can be introduced by removing 3 Sr^{2+} ions under the condition of charge balancing. But this will, in turn, create the +ve ion vacancy. As the creation of +ve ion vacancy required a good deal of energy the incorporation of Dy^{3+} will be limited. As a result phosphors prepared with charge compensator are less diamagnetic than those prepared without it as shown in fig. 3.9.

3.5 Optical Characterisation :

The strontium sulphate phosphors prepared in the present investigation were tested for their optical properties. First, an ultraviolet lamp (mineralite U.V.S. 12 USA) emitting predominately 3650 \AA° Hg doublet was used as an excitation source. It was found that phosphors do not exhibit fluorescence and thermoluminescence under UV excitation. However, the phosphors were found to show fluorescence, phosphorescence and thermoluminescence under X-ray excitation. This observation appears to indicate that the host lattice of $SrSO_4$ must be a high band gap material.

ob. No.	2θ : degree	θ : degree	Sin θ	h	K	l	Observed 'd' : cm	Calculated 'd' : cm	Relative intensity
1.	21.0	10.5	0.1822	0	0	1	4.23	4.231	12.28
2.	23.6	11.8	0.2044	1	1	1	3.77	3.769	26.31
3.	25.9	12.95	0.2241	0	0	2	3.433	3.438	28.070
4.	28.0	14.0	0.2419	1	0	2	3.177	3.185	52.631
5.	30.0	15.0	0.2588	2	1	1	2.972	2.977	87.719
6.	32.7	16.35	0.2815	1	1	2	2.731	2.731	69.648
7.	37.7	18.85	0.3230	1	2	1	2.388	2.385	29.824
8.	42.1	21.05	0.3591	2	2	1	2.141	2.145	38.596
9.	44.1	22.05	0.3754	1	2	2	2.045	2.052	100.00
10.	46.4	23.2	0.3939	4	1	0	1.947	1.956	26.315
11.	51.4	25.7	0.4336	3	0	3	1.769	1.776	29.824
12.	54.3	27.15	0.4563	4	1	2	1.691	1.688	24.561
				1	3	4			
13.	57.3	28.65	0.4794	2	3	0	1.604	1.607	33.33
14.	59.2	29.6	0.4939	2	3	1	1.569	1.560	22.806

TABLE NO. 3.1
SC₀₀ [Original Material (SrSO₄)]

ob. No. :	2θ : degree :	θ : degree :	Sin θ :	h :	k :	l :	Observed 'd' : cm :	Calculated 'd' : cm :	Relative intensity :
1.	28.2	14.1	0.2436	1	0	2	3.177	3.162	35.82
2.	32.9	16.45	0.2831	1	1	2	2.731	2.721	35.82
3.	33.6	16.8	0.2890	0	2	0	2.674	2.666	32.835
4.	37.9	18.95	0.3247	2	1	2	2.377	2.372	19.402
5.	40.0	20.0	0.3420	2	2	0	2.253	2.252	14.925
6.	42.2	21.1	0.3599	2	2	1	2.141	2.140	31.343
7.	44.4	22.2	0.3778	1	1	3	2.041	2.039	67.163
8.	45.4	22.7	0.3859	4	0	1	1.999	1.996	100.0
9.	46.8	23.4	0.3971	4	1	0	1.947	1.940	22.387
10.	49.1	24.55	0.4154	3	2	1	1.857	1.854	13.432
11.	57.5	28.75	0.4809	4	2	1	1.601	1.601	29.850
12.	59.4	29.7	0.4954	1	3	2	1.555	1.555	17.910
				5	1	1			
13.	62.9	31.95	0.5291	5	1	2	1.447	1.456	25.373
14.	67.4	33.7	0.5548	5	2	1	1.388	1.388	16.417

Calculated lattice parameters for SC₀₁ } {
 ao = 8.329A° bo = 5.332A° co = 6.864A°

TABLE NO. 3.2
 SC₀₁ [Heat treated SrSO₄]

ob. No.	2θ : degree	θ : degree	Sin θ	h	k	l	Observed 'd' : cm	Calculated 'd' : cm	Relative intensity
1.	24.0	12.0	0.2029	1	1	1	3.77	3.797	24.46
2.	27.5	13.75	0.2368	2	1	0	3.295	3.253	76.59
3.	33.2	16.6	0.2875	0	2	0	2.674	2.696	62.76
4.	38.0	19.0	0.3256	2	1	2	2.377	2.366	19.14
5.	40.2	20.1	0.3437	2	2	0	2.253	2.241	17.02
6.	42.4	21.2	0.3616	2	2	1	2.141	2.130	34.57
7.	44.45	22.22	0.3778	1	1	3	2.041	2.039	100.00
8.	45.24	22.6	0.3843	2	0	3	2.006	2.004	88.29
9.	46.8	23.4	0.3971	4	1	0	1.947	1.940	17.02
10.	51.8	25.9	0.4368	3	0	3	1.769	1.763	23.40
11.	54.8	27.4	0.4602	3	1	3	1.679	1.674	17.02
12.	56.2	28.1	0.4710	2	3	0	1.640	1.635	10.63
13.	59.4	29.7	0.4955	1	3	2	1.555	1.554	14.89
14.	63	31.5	0.5225	3	2	3	1.475	1.474	35.10

Calculated lattice parameters for SC_{03} }
 $ao = 8.3153A^\circ$, $bo = 5.392A^\circ$, $Co = 6.8518A^\circ$ {

TABLE NO. 3.3
 SC_{03} [SrSO₄:0.1 wt% Dy]

ob. No. :	2θ : degree :	θ : degree :	Sin θ :	h :	k :	l :	Observed 'd', cm :	Calculated 'd', cm :	Relative intensity :
1.	28.2	14.1	0.2436	1	0	2	3.177	3.162	54.76
2.	30.1	15.05	0.2596	2	1	1	2.972	2.967	95.236
3.	32.8	16.4	0.2823	1	1	2	2.731	2.729	59.522
4.	33.5	16.75	0.2881	0	2	0	2.674	2.673	49.998
5.	37.7	18.85	0.3230	1	2	1	2.388	2.385	26.189
6.	39.9	19.95	0.3411	2	1	2	2.253	2.258	19.047
7.	42.1	21.05	0.3591	2	2	1	2.141	2.145	33.332
8.	44.2	22.1	0.3762	1	1	3	2.041	2.048	100.00
9.	45.2	22.6	0.3842	2	0	3	2.006	2.005	95.236
10.	46.3	23.15	0.3981	4	1	0	1.947	1.935	26.189
11.	51.6	25.8	0.4352	3	0	3	1.769	1.770	28.571
12.	62.6	31.3	0.5195	3	2	3	1.475	1.483	33.33
13.	64.2	32.1	0.5313	3	2	3	1.475	1.450	14.285
14.	65.2	32.6	0.5387	1	2	4	1.424	1.430	19.047

Calculated lattice parameter for SC_{38} } {
 $ao = 8.4185A^\circ$, $bo = 5.354A^\circ$; $Co = 6.822A^\circ$

TABLE NO. 3.4
 SC_{38} [SiSO₄ : 0.1 wt.% Tb]

ob No. :	2θ : degree :	θ : degree :	Sinθ :	h :	k :	l :	Observed 'd' : cm :	Calculated 'd' : cm :	Relative intensity :
1.	28.0	14.0	0.2419	1	0	2	3.177	3.185	33.33
2.	41.2	20.6	0.3518	1	0	3	2.208	2.192	28.571
3.	45.3	22.65	0.3851	2	0	3	2.006	2.000	100.00
4.	58.5	29.25	0.4886	2	3	1	1.569	1.576	33.53
5.	60.2	30.1	0.5015	2	1	4	1.527	1.536	33.33
6.	63.6	31.8	0.5269	3	2	3	1.475	1.462	33.33

Calculated lattice parameters for SC₁₁ } { ao = 8.451A°, bo = 5.259A°, Co = 6.808A°

TABLE NO. 3.5

SC₁₁ [SrSO₄ : 0.1 wt. % Tb]

Phosphors	SC ₀₃	SC ₀₆	SC ₁₀	SC ₃₀	SC ₃₃	SC ₃₇	SC ₁₁	SC ₁₄	SC ₁₆	SC ₄₁	SC ₄₃
Electrical Conductance	1.579	1.538	1.666	1.666	1.5	1.428	1.578	1.666	1.724	1.428	1.6

TABLE NO. 3.6

Electrical conductance (dI/dv) x 10⁻⁷ of different SrSO₄ phosphors for different concentrations.

FIGURE CAPTIONS

- 3.1 X-ray diffraction patterns for SC_{00} , SC_{01} , and SC_{03} phosphors.
- 3.2 X-ray diffraction patterns for SC_{11} and SC_{38}^* phosphors.
- 3.3 I-V curve for typical phosphors SC_{16} , SC_{14} and SC_{11} .
- 3.4 I-V curves for phosphors SC_{10} , SC_{37}^* and SC_{16} , SC_{43}^* .
- 3.5 Plots of logarithmic current versus logarithmic voltage for typical phosphors SC_{10} and SC_{16} .
- 3.6 Schematic circuit and sample holder diagram of two probe resistivity apparatus.
- 3.7 I-V curves for typical phosphors SC_{01} , SC_{03} , and SC_{30}^* .
- 3.8 Schematic diagram of the set used for measurement of thermoelectric power.
- 3.9 Experimental set-up for susceptibility measurement.
- 3.10 Magnetic susceptibility of $SrSO_4:Dy$ phosphors as a concentration of Dy.

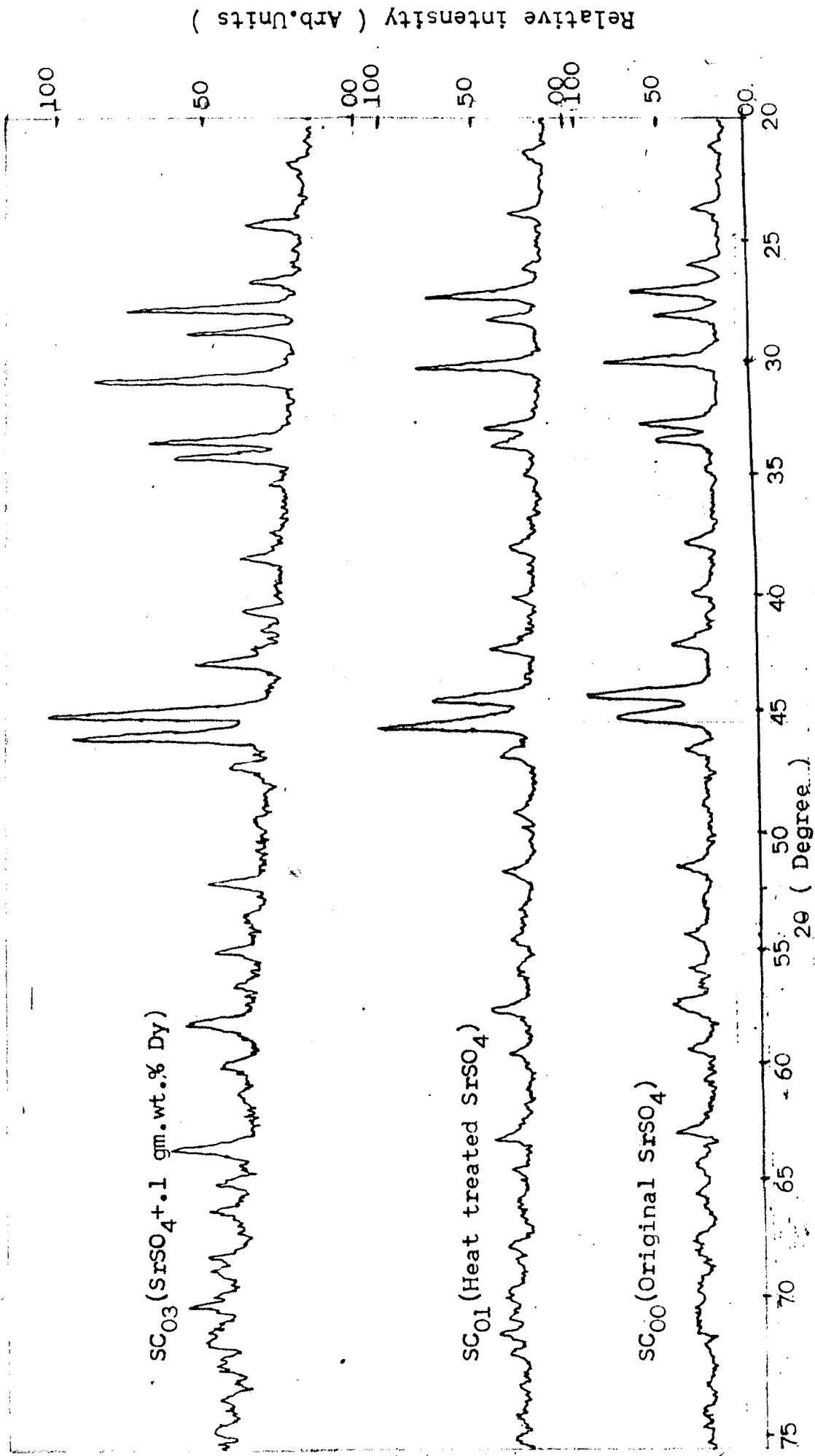
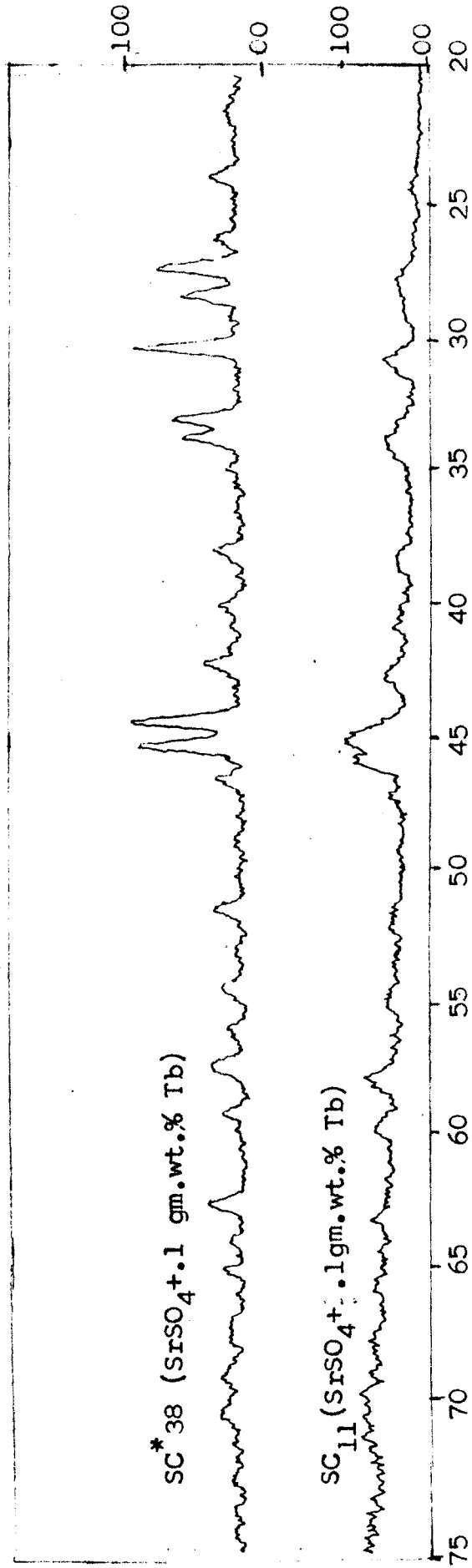


Fig:3.1 X - Ray Diffraction patterns for typical samples.

Relative Intensity (Arb. Units)



2θ (Degree)

Fig : 3.2 X - Ray Diffraction patterns for typical samples.

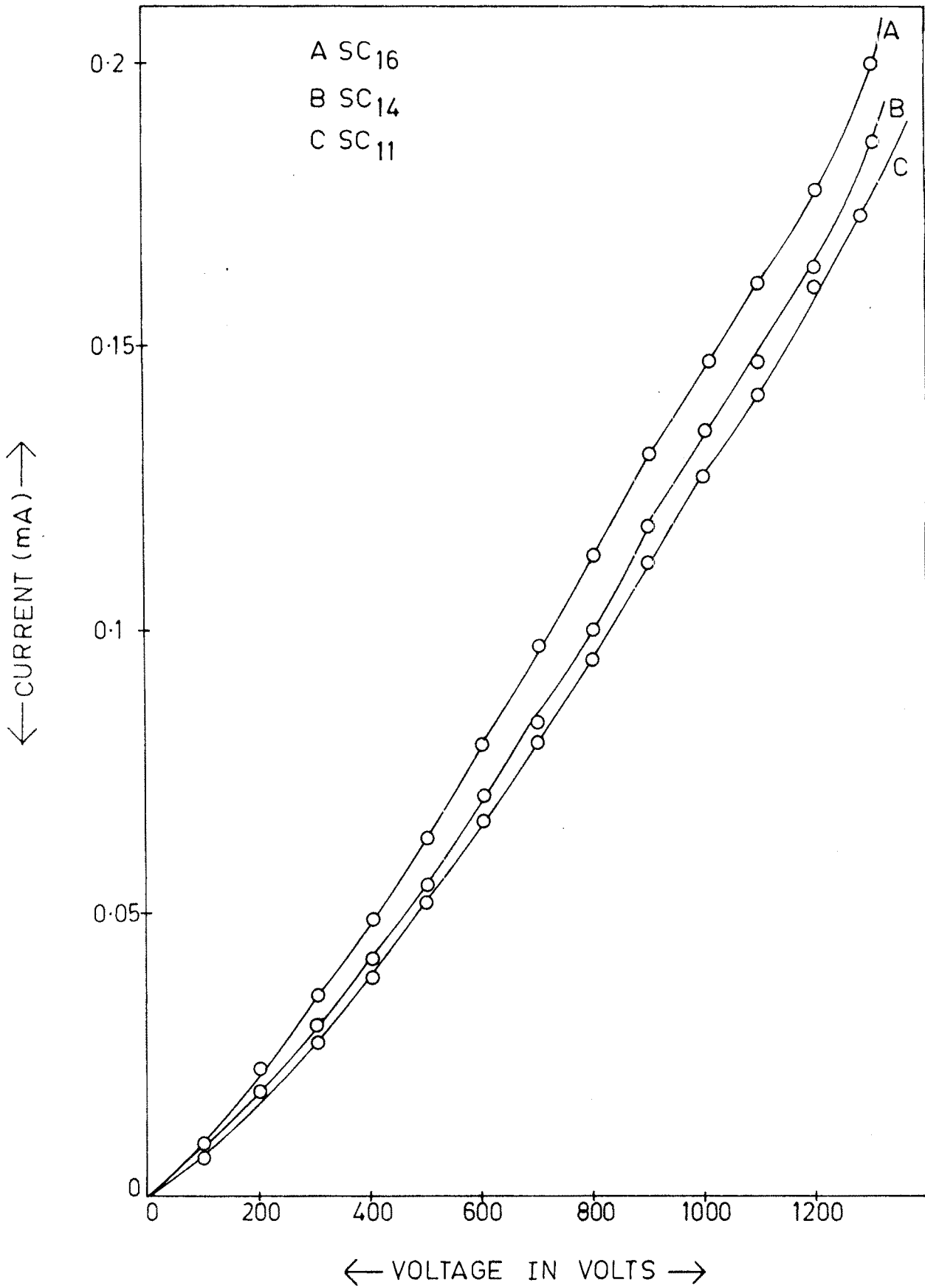


FIG: 3.3

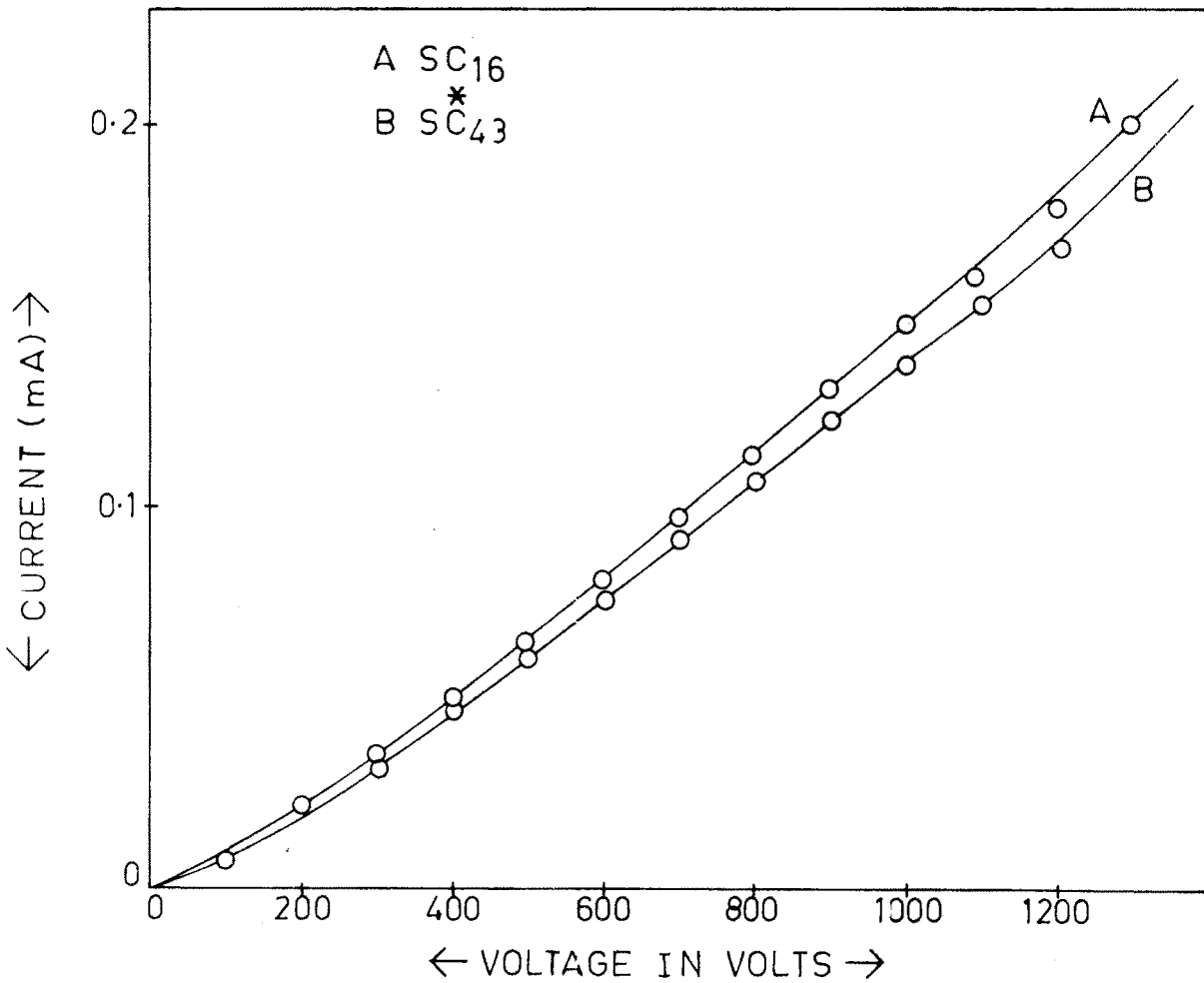
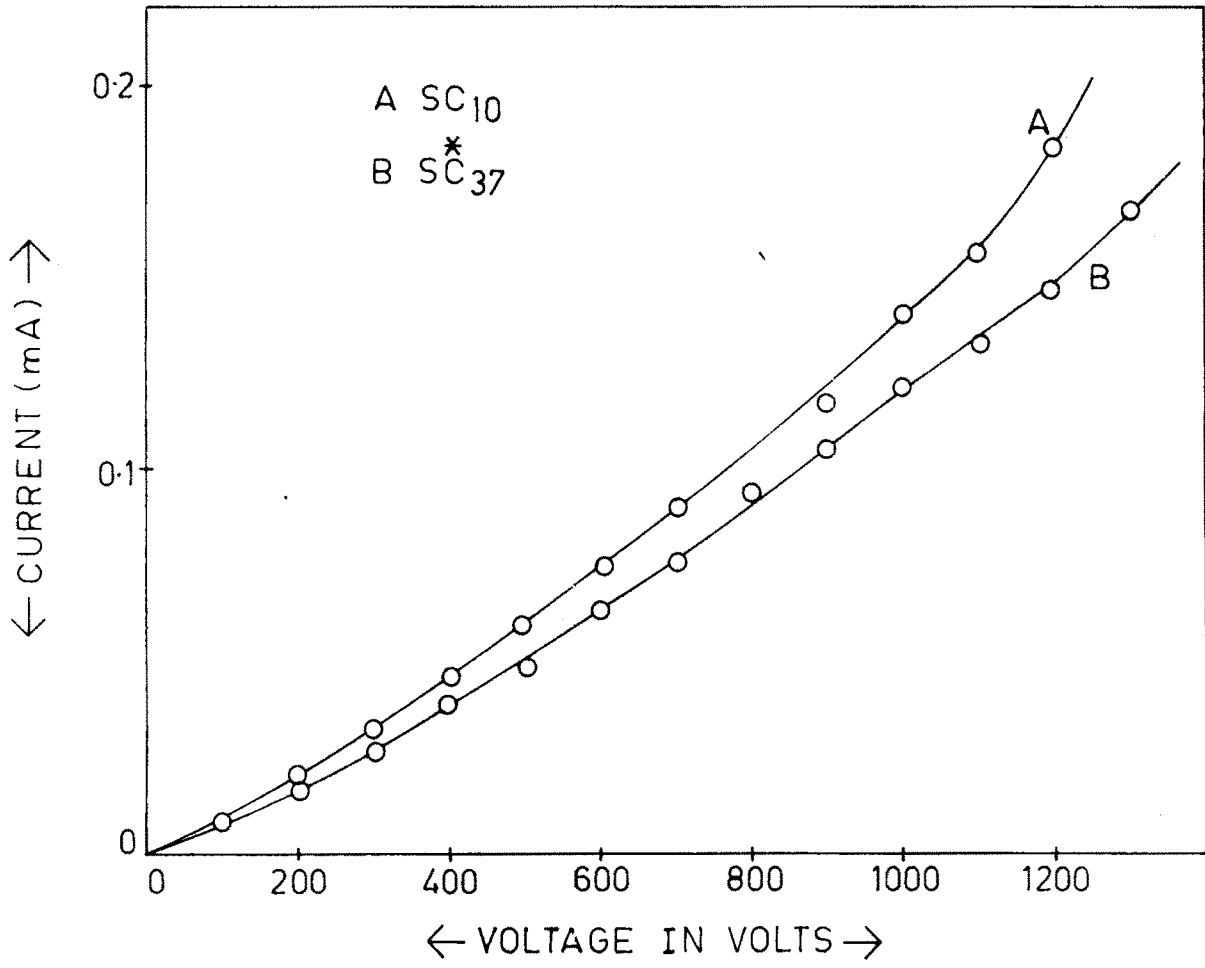


FIG: 3.4

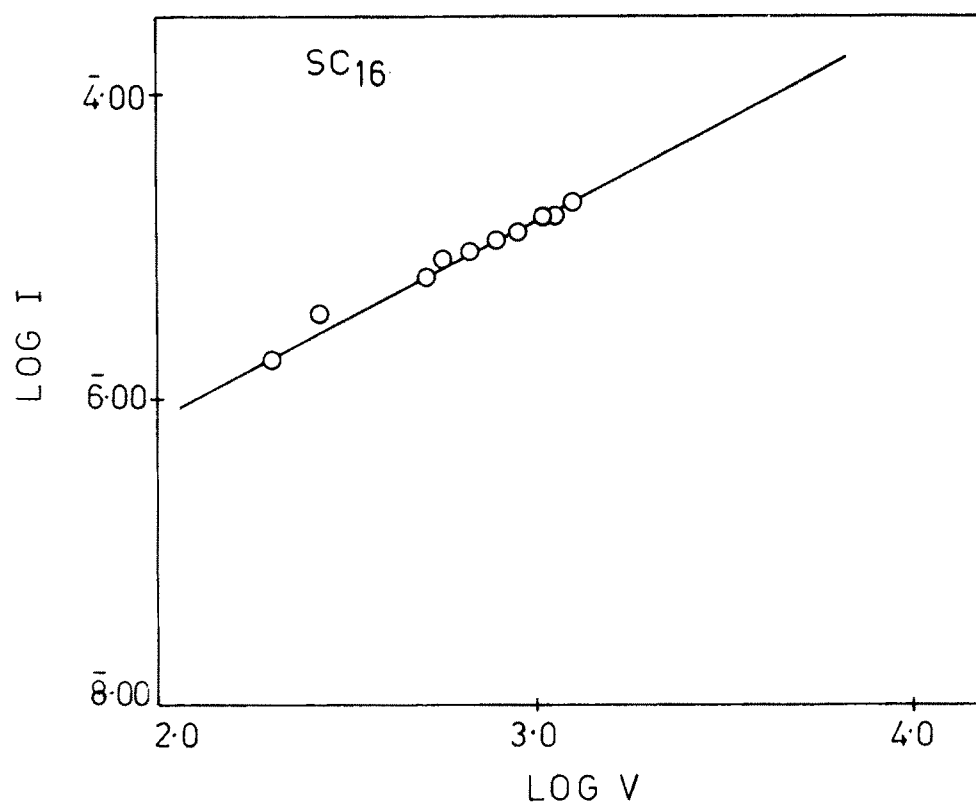
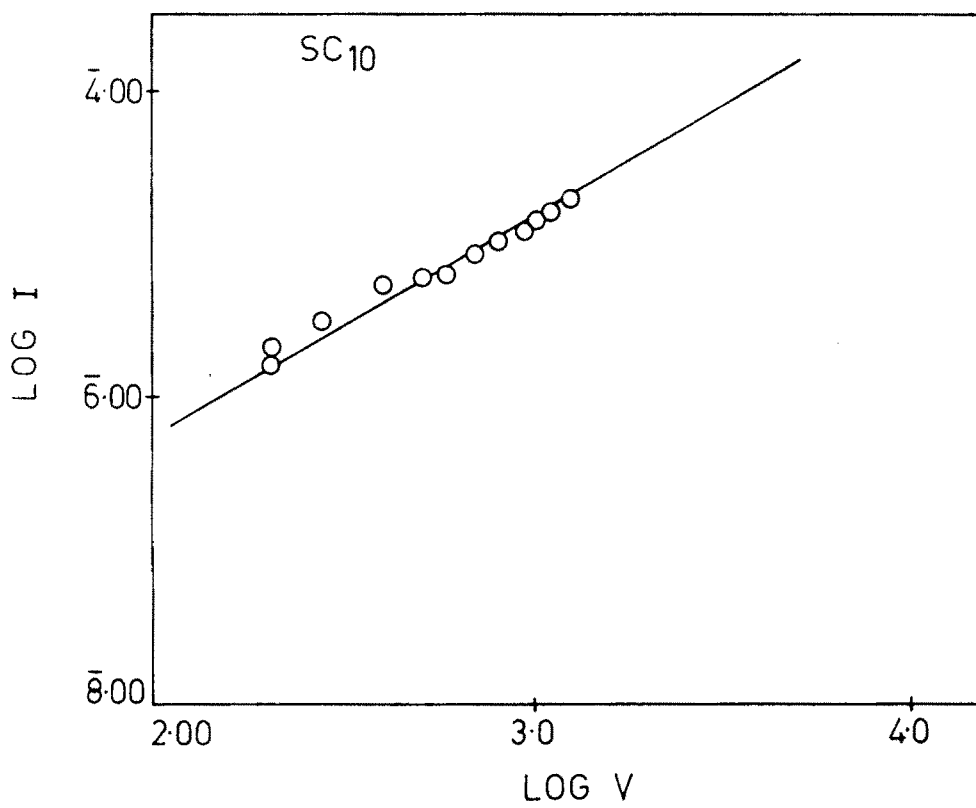


FIG: 3.5

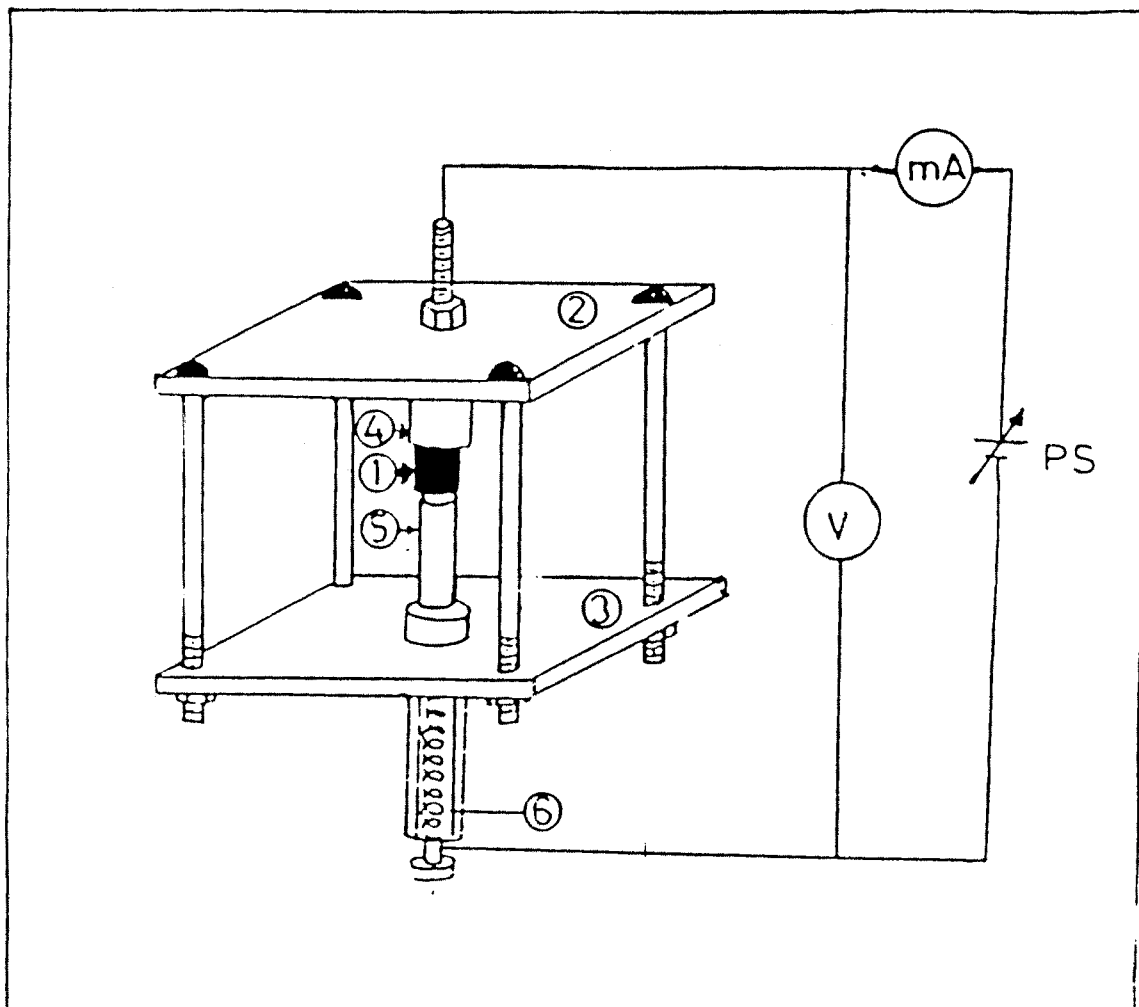


FIG: 3.6

FIG. NO. 3.6

- 1 - sample in pellete form.
- 2 - perspex sheet on which upper electrode is fitted
- 3 - perspex sheet on which lower electrode is fitted.
- 4 - upper electrode.
- 5 - lower electrode
- 6 - spring to hold the pellete under mild pressure.

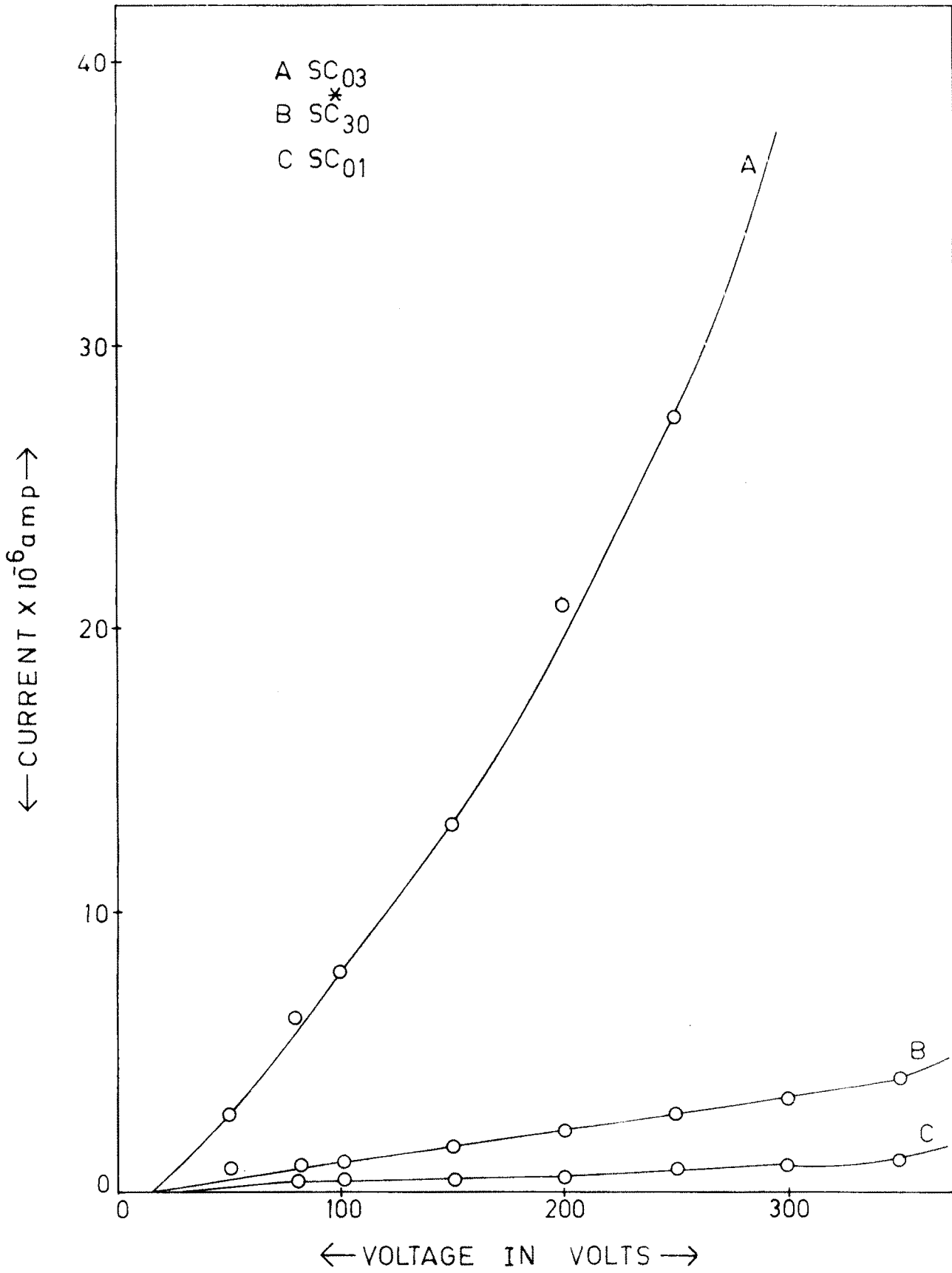


FIG: 3.7

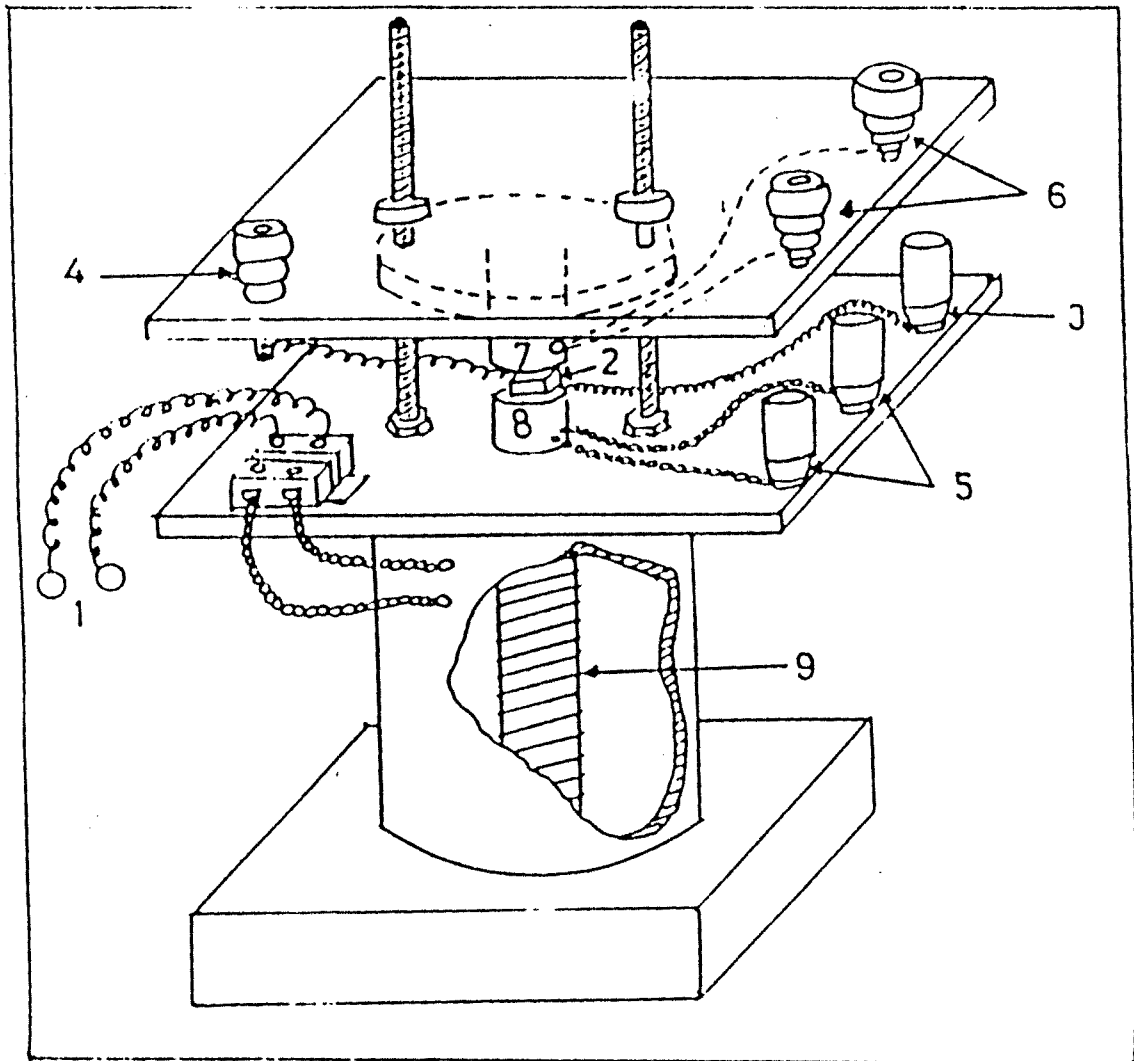


FIG NO. 3.8

Schematic diagram of the experimental set-up for thermoelectric power measurements.

- 1 - Connecting wires to heater.
- 2 - Sample in the pellete form.
- 3 - Lower electrode terminal.
- 4 - Upper electrode terminal.
- 5 - Thermocouple attached to lower electrode.
- 6 - Thermocouple attached to upper electrode.
- 7 - Upper electrode.
- 8 - Lower electrode.
- 9 - Heating coil surrounding the lower electrode.

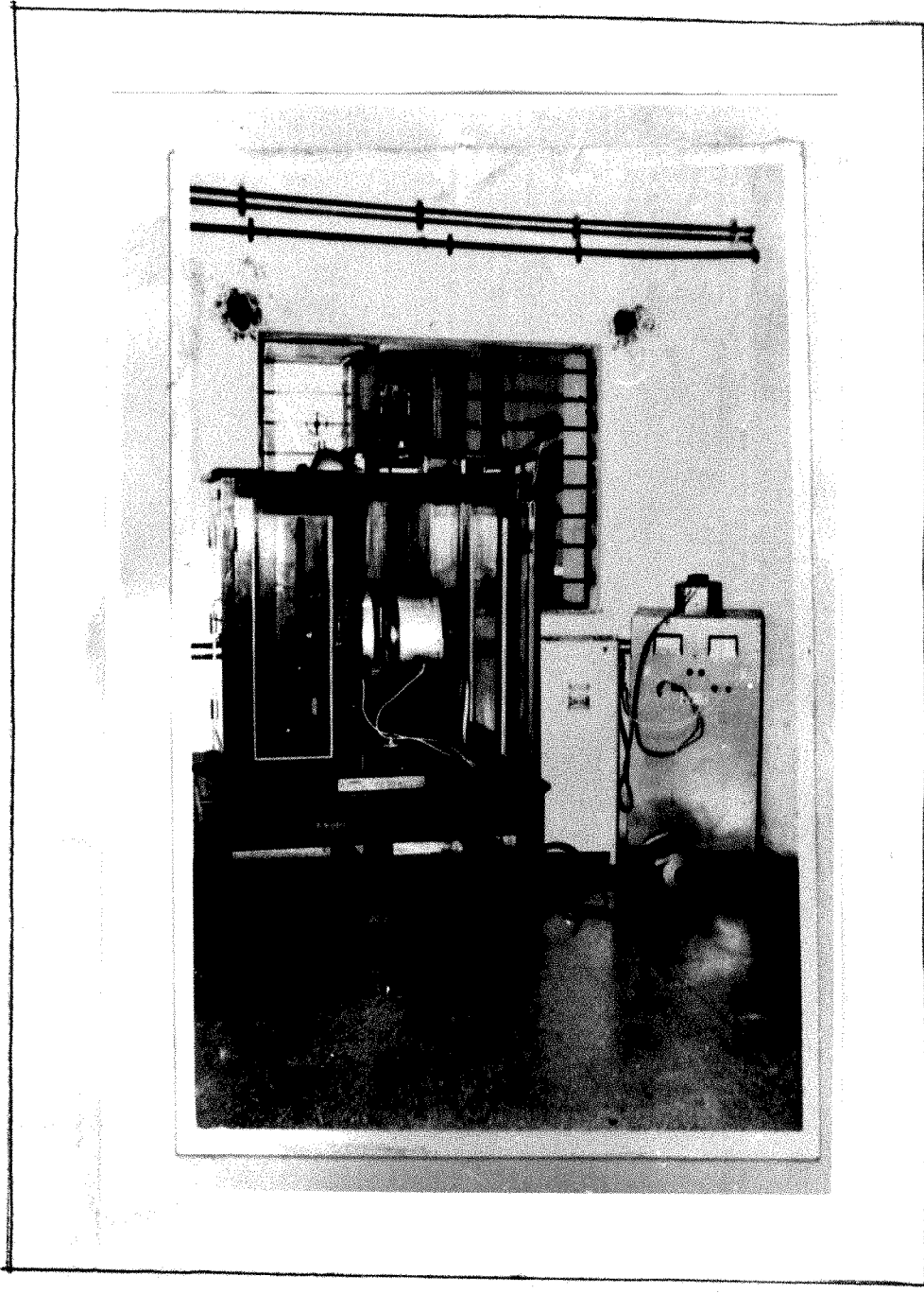


FIG. NO. 3.9

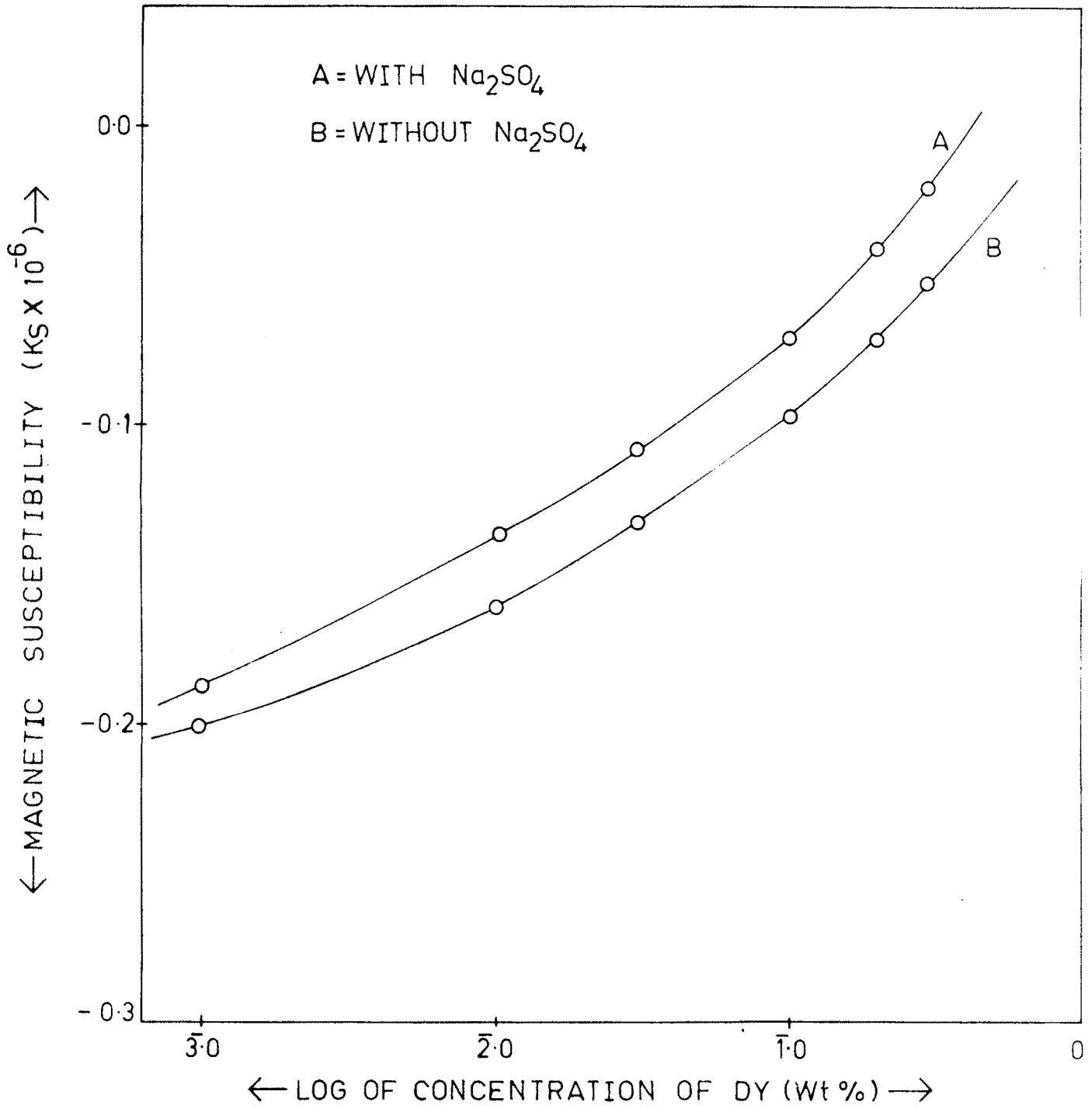


FIG:3.10

REFERENCES

1. Hand book of Chemistry and Physics, 50th edition, Editor - Robert C. Weast. Ph.D.
2. Lantana, R.F. and Martinelli M., Phys. Stat. Sol. (a), 11, 343 (1972).
3. Nambi K.S.V., Bapat V.N., and Ganguly, A.K., J. Phys. C, Solid State Phys., 7, 4403 (1974).
4. Mulla M.R. and Pawar, S.H., Pramana, 12, 593 (1979)
5. Rao, R.P., Journal of Mat. Sci., 21, 3357-3386 (1986).
6. Mott. N.F. and Gurney R.W. 'Electronic Processes in Ionic Crystals'. Dover Publications, INC.(New York) P-172, (1940).
7. Ebert I and Teltow, J. Ann. Phys. 15, 268 (1955).
8. Ramsastry C. and Murty Y.V.G.S. Proc., Roy. Soc., 305, 441 (1968).
9. Robert R., Heikes and Roland W, Thermoelectricity science and engineering Ure, Sr. Interscience Publishers (New York) P-88 (1961).
10. Jagadale S.H. and Pawar S.H., Bull. Mater. Sci. Vol.-5, No. 5, 390 (Dec. 1983).
11. Jensen P. Ann. De. Physik, 34, 161 (1939).
12. Bowers R. and Melamed. N.T., Phys. Rev. 99, 1781, (1975).
13. Johnson P.D., and William F.E., J. Chem., Phys., 17, 435, (1949).

14. Johnson P.D. and William F.E.J. Chem. Phys. 18, 323 (1950).
15. Mulla M.R. and Pawar S.H., Mat. Res., Bull. 12, 929 (1977).
16. Mulay L.N. Magnetic Susceptibility, Interscience Publishers, New York. P. 1838 (1963).
17. Gouy, L.G. Compt. rend 109, 935 (1889).
18. Heer C.V. and Rausch C. Phys. Rev. 90, 530 (1953).
19. Nambi K.S.V. Bapat, V.N. and Ganguly A.K.J. Phys., C. Solid State Physics, 7, 4404 (1974).
20. Kroger F.A. and Hellingmann, J.E., J. Electrochem. Soc. 95, 68 (1949).